

# Global maps of Rayleigh wave attenuation for periods between 40 and 150 seconds

Magali BILLIEN and Jean-Jacques LÉVÊQUE

Institut de Physique du Globe (Université Louis Pasteur and CNRS), Strasbourg, France

Jeannot TRAMPERT

Department of Geophysics, Utrecht University, The Netherlands

**Abstract.** Studies of seismic attenuation must account for the large amplitude deviations caused by elastic focusing of energy. In a new approach, we jointly invert phase and amplitude measurements of 19,000 minor arc Rayleigh waves between periods of 40 and 150 seconds. The simultaneous inversion ensures that attenuation and phase velocity are mutually consistent because the phase and focusing term of amplitude are modelled using a common elastic model. At the shortest periods the maps show a good correlation between attenuation and phase velocity, suggesting a common cause in the uppermost mantle, most probably thermal in origin. This correlation is lost at longer periods. The main signal beyond periods of 100 seconds is a strongly attenuating circum Pacific zone and a pronounced ring of high attenuation around Africa. This feature seems reliable in our attenuation maps but not correlated to an equivalent structure in phase velocity. We thus favour scattering of wave energy on large size structures as a possible cause.

## Introduction

Attenuation of seismic waves gives access to the anelastic properties of the Earth resulting in complementary geodynamical information to that obtained from elastic properties. The purpose of this work is to map attenuation of surface waves at different periods to obtain, at a later stage, a 3-D model of the quality factor  $Q$  inside the Earth.

The first determinations of quality factors along paths associated to pure tectonic provinces (e.g. ocean, shield) showed a correlation between phase velocity variations and quality factor variations and the existence of large differences between quality factors beneath continents and oceans [Ben-Menahem, 1965; Nakanishi, 1979; Mills and Hales, 1978; Dziewonski and Steim, 1982].

Moreover, the attenuation in the upper mantle is thought to present large lateral variations [Canas and Mitchell, 1978; Lee and Solomon, 1979; Nakanishi, 1979; Sipkin and Jordan, 1980; Bussy et al., 1993; Durek et al., 1993; Romanowicz, 1995] at local and global scale. Global studies from normal modes [Romanowicz et al., 1987; Smith and Masters, 1989; Roult et al., 1990] and surface wave analyses along great circle paths [Durek et al., 1988, 1989, 1993; Romanowicz, 1990, 1994, 1995] led to frequency dependent quality factor maps  $Q_{Rayleigh}(\omega)$  and  $Q_{Love}(\omega)$ . Obtained at periods greater than 100 s, these maps showed the existence of a strong degree 2 in attenuation anti-correlated with phase velocity [Romanowicz et al., 1987; Smith and Masters, 1989]. Romanowicz [1995] located the source of this degree 2 in the transition zone, for both attenuation and phase velocity,

while Durek et al. [1993], studying degrees 2, 4 and 6 favoured the source of attenuation at shallower depth in the low velocity zone. Working with data at shorter periods is expected to constrain this depth location better.

The amplitude of surface waves depends not only on the quality factor (which in turn depends on anelastic attenuation and scattering), but also on the geometrical spreading and the focusing effect. Geometrical spreading is due to the conservation of surface wave energy on a spherical Earth. The focusing effect is due to lateral variations in phase velocity which focus and defocus the beam of rays [Woodhouse and Wong, 1986]. Wong [1989] exploited this connection first and used amplitude measurements as additional constraints for phase velocity modelling.

While geometrical spreading is well known and easy to model, the focusing effect is much more difficult to take into account and several methods have been proposed to model it in quality factor determinations. Without introducing a priori knowledge of a phase velocity model, focusing can be eliminated within the ray path approximation using combinations of multi-orbit paths [Romanowicz, 1990, e.g]. Using an a priori velocity model and exact ray theory, Durek et al. [1993] desensitised amplitude measurements prior to quality factor determinations. Romanowicz [1995] simply rejects paths where the comparison between first and second orbits show a suspiciously large amount of focusing. Each of these methods has its own difficulties and limitations and none is fully satisfactory. We chose not to correct the focusing effect but to include it in the inversion instead. We adopt a path integral approach where focusing depends on phase velocity variations along and perpendicular to the path [Woodhouse and Wong, 1986]. We then jointly invert phase and amplitude measurements for phase velocity and attenuation. This ensures consistent maps of quality factor and phase velocity, and we do not have to reject data with significant focusing. With our data set alone, we cannot separate the effects of scattering and anelastic attenuation. The results of our quality factor determinations include thus both. However, scattering is mostly expected to decrease the wave amplitude if constructive interferences are neglected, as done in the widely used first Born approximation. For this reason, scattering is not likely to explain high  $Q$  anomalies.

## Data and Method

We use the extensive data set of amplitude and phase measurements from fundamental mode surface waves compiled by Trampert and Woodhouse [2000]. Compared to previous measurements by the same authors, the technique has been refined by starting from an aspherical reference model. For a detailed description of the automatic measurement technique and implementation of the strict data rejection criteria, see Trampert and Woodhouse [1995]. Throughout this work, we assume that the path integral approximation is valid. We use here for the first time the amplitude measurements which are more sensitive to off-path effects than phase data. Most data affected by multi-pathing have al-

Copyright 2000 by the American Geophysical Union.

Paper number 2000GL011389.  
0094-8276/00/2000GL011389\$05 00

ready been eliminated at the measuring stage by, among others, identifying notches in the spectrum. Using a realistic phase velocity model, we compared focusing predictions from path integral and full ray theoretical calculations. For minor arcs, 96 % of the data were adequately modelled by the path integral approach. This percentage quickly decreases for higher order orbits. We thus chose to eliminate all major arc measurements from the initial data set. We further compared measurements for the same paths made on 1 sps and 0.1 sps channels. The long period channels systematically showed deviations at the shortest periods (40 s) due to filters modifying amplitudes around the Nyquist frequency. We thus further eliminated all measurements done on 0.1 sps channels. We are then left with 19,000 paths corresponding to amplitude and phase measurements for fundamental mode Rayleigh waves between periods of 40 and 150 seconds.

We designed a joint inversion of phase and amplitude measurements to simultaneously obtain phase velocity and quality factor maps for fundamental mode surface waves. Phase velocity and quality factor are expanded in terms of spherical harmonics up to degree 20. The observed phase of a surface wave is related to the phase velocity along the path by :

$$\Phi(\omega) = \Phi_0(\omega) + \Phi_{inst}(\omega) + \int_{path} \frac{\omega}{c(\omega, s)} ds \quad (1)$$

where  $\Phi_0$  is the initial source phase due to the rupture process,  $\Phi_{inst}$  is the instrumental phase shift,  $k$  is the wave number and  $c$  is the local phase velocity along the path. At this stage we assume source (taken from the Harvard catalogue) and instrumental phases perfectly known. If  $A_0$  is the amplitude at the source and  $R_{inst}$  is the amplitude response of the instrument, we may write the observed amplitude  $A(\omega)$  as a function of the derivatives of  $c$  parallel ( $\partial_{\parallel}^2 c$ ) and perpendicular ( $\partial_{\perp} c$ ) to the path:

$$A(\omega) = A_0(\omega) R_{inst}(\omega) F(\partial_{\perp} c, \partial_{\parallel}^2 c) e^{-\int_{path} \frac{\omega}{2cQ} ds} \quad (2)$$

$F(\partial_{\perp} c, \partial_{\parallel}^2 c)$  is the focusing term. Expressing all quanti-

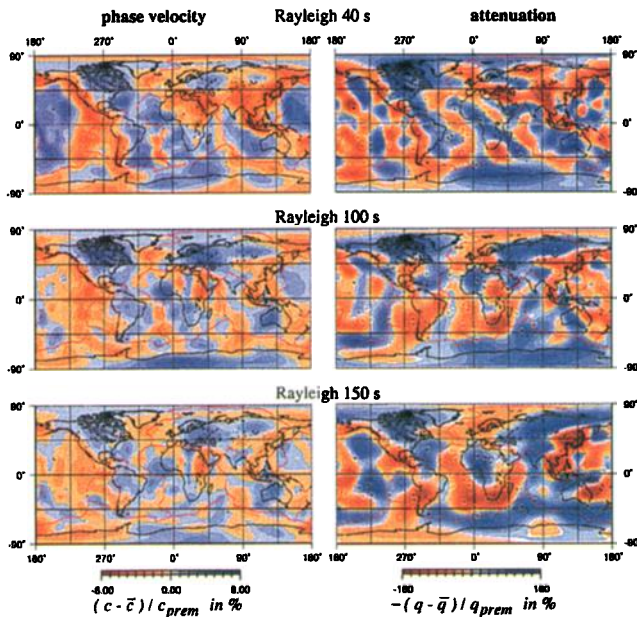


**Figure 1.** (left) phase velocity maps; (right) attenuation maps obtained by a simultaneous inversion ( $q = 1/Q$ ). The mean value is removed.

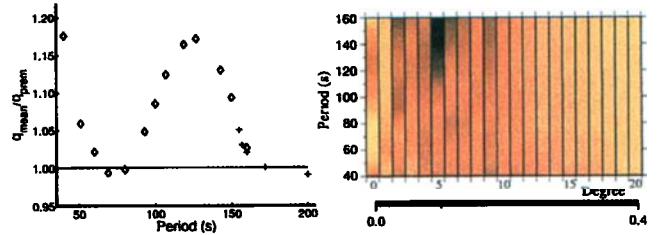


**Figure 2.** (left) Mean values of the attenuation factor represented by the  $q_{mean}/q_{prem}$  ratio. This study ( $\diamond$ ) and values from Durek and Ekström [1996] (+); (right) Energy spectrum, as a function of degrees, at periods between 40 and 160 sec.

ties as perturbations to surface wave seismograms calculated from PREM (put reference here), we may write :

$$\begin{cases} d\Phi(\omega) &= \int_{path} \omega \frac{dn}{n_0(\omega, s)} ds \\ \ln(dA(\omega)) &= F(\partial_{\perp} c, \partial_{\parallel}^2 c) \\ -\frac{\omega n_0 q_0}{2} \int_{path} (\frac{dq}{q_0} + \frac{dn}{n_0} \frac{dq}{q_0}) ds \end{cases} \quad (3)$$

with  $dn = n - n_0$  the local phase slowness perturbation and  $dq = q - q_0 = 1/Q - 1/Q_0$  the local perturbation in attenuation. Explicit expressions for  $F$  are given in Woodhouse and Wong [1986].

The cross term  $dq \cdot dn$  is usually neglected. To check this assumption, we computed synthetic data using arbitrary, but realistic, attenuation and phase models. For each path, we evaluated the relative amplitude difference between synthetic data keeping the cross term in equation (3) and neglecting it. Most of the obtained differences are less than 1 %, and nearly all of them are less than 4 %. This is much below the 30 % uncertainty we believe to be present in our amplitude data. Neglecting the cross-term will thus not significantly bias our inversions, and inverting the linear system (3) at several periods is now straightforward. Including the focusing term is crucial for quality factor determinations. Tests made on synthetic amplitude data alone show that almost all effects due to focusing can be explained by  $Q$ . The issue of simultaneous inversion versus correcting amplitude data from focusing effects prior to inversion is less critical, especially at the length scales involved in this study. We simply prefer the simultaneous inversion which guarantees the consistency between attenuation and phase velocity models. The 30 % data errors on amplitude mentioned above were found by looking at the same events recorded at very close stations, and comparing close and similar events recorded at a same station. If we want to reconcile these incompatible amplitude data, we would necessarily have to include event and station terms in our inversion procedure, thus introducing new degrees of freedom in the theory. In this paper, we prefer not to use these event and station terms in order to keep a better constraint on the inversion process. The expected drawback is a poor variance reduction due to the presence of these incompatible data that our theory cannot take into account. Not surprisingly, the quality factor maps and phase velocity maps give variance reductions ranging from 10 to 25 % for amplitude data (from low to high frequencies) and from 30 to 90 % for phase data. We

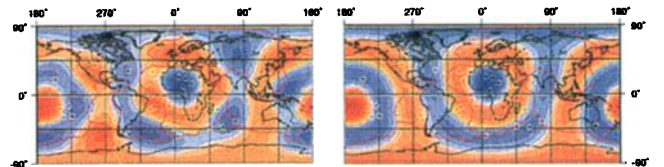


**Figure 3.** Rayleigh 150 s (left) degree 5 only; (right) component  $Y_5^0$  rotated of degree 5 only.

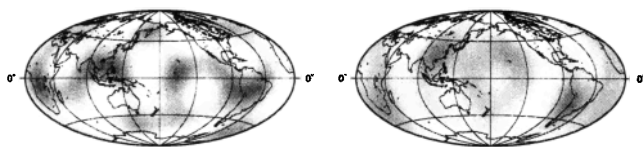


**Figure 4.** (left) Durek *et al.*'s (1993) results at 160 seconds; (right) our filtered model (degrees 2, 4, 6 only) at the same period.

show phase velocity and attenuation maps (Figure 1), but we only discuss attenuation because phase velocity maps are very similar to those published in *Trampert and Woodhouse* [2000] with correlation coefficients better than 0.8.

## Results

Figure 1 displays phase velocity and attenuation maps at three representative periods. An examination of the results at shorter intervals in period shows that the maps are quite coherent from one period to the next, even if it is not apparent on this simplified figure.

The coherence between phase velocity and attenuation is most pronounced at shorter periods. At 40 seconds, low velocity areas generally correspond to high attenuation areas, and most high velocity areas, like continental shields, correspond to low attenuation areas. Several discrepancies however exist. The Hawaii and Emperor seamounts and the Southern Pacific appear as very attenuating with corresponding high velocities. Most ridges (Medio-Atlantic, Central-East Indian, Central-East Pacific) appear as attenuating areas but only some of them, like the Pacific or East Indian ridges, appear as low velocity areas. Continental shields, like West Africa, North America, South America or East Australia, display weak attenuation and high velocities, while collision areas or active tectonic continental areas, like the Mediterranean area or Tibet, associate high attenuation and low velocities. At longer periods, this overall coherence between phase velocities and attenuation becomes less and less pronounced: between 50 and 80 s, the Eurasian plate is no longer attenuating; plate boundary areas like the subduction and strike-slip area along the western coast of North America, remain attenuating, while the attenuating pattern associated to ridges at short period vanishes progressively and disappears at periods greater than 80 seconds.

At 100 seconds, the main attenuating areas are located in subduction zones such as the Philippines, Japan, Kamchatka, Canada, South America, and beneath Europe, East Africa, and South Africa. In the period range 100-150 s, the ridges are no longer attenuating, neither is Tibet and Turkey, two tectonically active continental zones, while the subduction zones remain strongly attenuating. Another large attenuating area encompasses the Central Pacific, Eastern Australia and New-Zealand. The North American, Eurasian and African shields display rather low attenuations. The most remarkable changes in the attenuation pattern at longest periods is the high attenuation ring which builds up around Africa, and perhaps a westward migration of the high attenuation zone in North America.

Note that "blue" values higher than 100% on the maps lead to negative values of  $Q$ , meaning amplification rather than attenuation. While this cannot be completely excluded, it is still very unlikely since it would imply for example constructive scattering. In this study, we strongly favour another interpretation. Negative  $Q$  values are most probably due to the gaussian assumption made on the error statistics, which is clearly an over-simplification for positive parameters like  $Q$ .

In these maps, the average values (degree 0) have been removed. However, they carry an important information: the mean deviations from the 1-D reference model PREM.

The deviations of the Rayleigh fundamental mode quality factor ( $Q_R(\omega)$ ) are displayed on Figure 2-left as a function of period. The average  $q$  values we obtained are systematically greater than those found in PREM and is in agreement with the longer period study of *Durek and Ekström* [1996].

The rest of energy in the maps is theoretically spread over degrees 1 to 20, but due to the damping we used, degrees higher than 13 are strongly suppressed. Among the low, undamped degrees, degrees 2 and 5 are very energetic, especially at long periods (Figure 2-right). Degree 2 corresponds to two attenuating areas, located in the Southern Atlantic and Northwestern Pacific, except at 40 seconds where a four quadrant pattern is dominant, centered at  $0^\circ\text{N}-0^\circ\text{E}$ .

In our attenuation model at 160 s, the degree 2 pattern is not clearly correlated to the velocity degree 2, unlike what was found at the same period by *Romanowicz* [1990]. Unfortunately, the period range we share with this study is very small, and we cannot investigate this question further.

The energy present in degree 5 (Figure 3) mainly corresponds to a band-shaped pattern equivalent to the equatorial band of  $Y_5^0$  in a rotated reference frame where the poles correspond to Central Africa and Tonga-Kermadec. In this frame, the equator is close to the circum Pacific ring, which appears as a high attenuation zone. This can be understood as a signal from the concentration of subduction zones in this area. The red ring around the African continent is in fact the second red band of this pattern, the third one being concentrated at the Tonga-Kermadec pole. This African ring may thus be suspected to be only an artefact deriving from a main signal, the circum Pacific zone. However, such an equatorial band can be taken into account by the 0-component of any degree, and the secondary rings can easily be destroyed by interferences between other components of the same or others degrees. The fact that degree 5 is very energetic and that, among its 11 components, most of the energy goes on a  $Y_5^0$ -like term, suggests that the data are strongly compatible with this pattern, including the high attenuation African ring. In order to compare our results at long period to those of *Durek et al.* [1993], we filtered our model, keeping only degrees 2, 4 and 6 of the spherical harmonic development. We show both models on Figure 4 at the overlapping period of 160 s. We make the comparison at 160 s, which is the shortest period in *Durek et al.*'s [1993] study, and for which our results are more reliable than at period 200 s. The two models show good agreement: in both cases, low attenuation areas lay beneath East-Africa, India, Australia and near the Rodriguez triple junction; very attenuating zones are located beneath the Indian Ocean or Mexico. Some differences are present too, in Birmania, Central Pacific Ocean and Alaska.

## Discussion and conclusions

The existence of strong anomalies and the consistency between attenuation maps, velocity maps and tectonics at short periods (40s-80s) favour the idea that a large part of the attenuation we measure comes from sources in the lithosphere, directly related to geodynamical processes such as ridges and subductions. However, deeper sources of attenuation also clearly exist, since we still observe  $q$  anomalies at periods as large as 100-150 s. The subduction zones, steadily attenuating in the whole period range of the study, are certainly a major feature in the attenuation pattern of the Earth.

At 40 s period, we find a clear pattern of attenuation related to ridges which progressively vanishes at longer periods. This could be explained by relatively small but strongly attenuating zones, close to the surface, and a potential candidate is the presence of partial melt. Subduction zones have a small lateral extension, too, but they are known to be present at least down to 700 km. We observe a consistent attenuation pattern related to them up to our longest peri-

ods. Indeed, a 150 s Rayleigh wave has a penetration close to this depth, even though its maximum of sensitivity is at 250 km. The reason for observing subduction zones as attenuating is less clear. Among other possibilities, let us mention that slabs are generally observed as strong, localized, positive velocity contrasts in the tomographic images, and could therefore be a source of scattering for surface waves. This non-thermal origin for slab attenuation would have the advantage to explain the association between high velocities and strong attenuation, otherwise difficult to understand. Another region for which the scattering could play a major role in the observed attenuation is the Eurasia. Here the strong attenuation is observed only at short periods, and could be due to strong heterogeneities in the Eurasian crust and lithosphere. Accounting for focusing effects in the modelling of amplitudes allowed us to retrieve the quality factor at periods as short as 40 s, much shorter than in previous global tomographic Q studies. This improvement in determination of Q over a range of shorter periods reveals new features in the attenuation pattern of the Earth and should lead to a 3-D Q-model with an enhanced depth resolution.

**Acknowledgments.** We thank John Woodhouse for his ray tracing code and an anonymous reviewer for his constructive comments. Studies like this one would not be possible without the dedicated efforts of many people at IRIS and GEOSCOPE. All plots, except 2-left, have been created with GMT software.

## References

- Ben-Menahem, A., Observed attenuation and Q values of seismic surface waves in the upper mantle, *J. Geophys. Res.*, **70**, 4641–4651, 1965.
- Bussy, M., J.-P. Montagner, and B. Romanowicz, Tomographic study of upper mantle attenuation in the Pacific Ocean, *Geophys. Res. Lett.*, **20**, 663–666, 1993.
- Canas, J. A., and B. J. Mitchell, Lateral variation of surface wave anelastic attenuation across the Pacific, *Bull. Seism. Soc. Am.*, **68**, 1637–1650, 1978.
- Durek, J. J., and G. Ekström, A radial model of anelasticity consistent with long-period surface-wave attenuation, *Bull. Seism. Soc. Am.*, **86**, 144–158, 1996.
- Durek, J. J., A. M. Dziewonski, and J. H. Woodhouse, Even order global distribution of the quality factor Q by inversion of surface wave amplitude data, *Eos Trans. Am. Geophys. Un.*, **69**, 397, 1988.
- Durek, J. J., M. H. Ritzwoller, and J. H. Woodhouse, Estimating aspherical Q in the upper mantle using surface wave amplitude data, *Eos Trans. Am. Geophys. Un.*, **70**, 1212, 1989.
- Durek, J. J., M. H. Ritzwoller, and J. H. Woodhouse, Constraining upper mantle anelasticity using surface wave amplitude anomalies, *Geophys. J. Int.*, **114**, 249–272, 1993.
- Dziewonski, A. M., and J. M. Steim, Dispersion and attenuation of mantle waves through waveform inversion, *Geophys. J. R. astr. Soc.*, **79**, 503–527, 1982.
- Lee, W. B., and S. C. Solomon, Simultaneous inversion of surface wave phase velocity and attenuation: Rayleigh and Love waves over continental and oceanic paths, *Bull. Seism. Soc. Am.*, **69**, 65–95, 1979.
- Mills, J., and A. Hales, Great circle Rayleigh wave attenuation and group velocity, part III, Inversion of global average group velocity and attenuation coefficients, *Phys. Earth Planet. Int.*, **17**, 307–322, 1978.
- Nakanishi, I., Phase velocity and Q of mantle Rayleigh waves, *Geophys. J. R. astr. Soc.*, **58**, 35–59, 1979.
- Romanowicz, B., The upper mantle degree 2 : Constraints and inferences from global mantle wave attenuation measurements, *J. Geophys. Res.*, **95**, 11,051–11,071, 1990.
- Romanowicz, B., On the measurement of anelastic attenuation using amplitudes of low-frequency surface waves, *Phys. Earth Planet. Int.*, **84**, 179–191, 1994.
- Romanowicz, B., A global tomographic model of shear attenuation in the upper mantle, *J. Geophys. Res.*, **100**, 12,375–12,394, 1995.
- Romanowicz, B., G. Roullet, and T. Kohl, The upper mantle degree two pattern: constraints from GEOSCOPE fundamental spheroidal mode eigenfrequency and attenuation measurements, *Geophys. Res. Lett.*, **14**, 1219–1222, 1987.
- Roullet, G., B. Romanowicz, and J.-P. Montagner, 3-D upper mantle shear velocity and attenuation from fundamental mode free oscillation data, *Geophys. J. Int.*, **101**, 61–80, 1990.
- Sipkin, S. A., and T. H. Jordan, Regional variation of Qscs, *Bull. Seism. Soc. Am.*, **70**, 1071–1102, 1980.
- Smith, M. F., and G. Masters, Aspherical structure constraints from normal mode frequency and attenuation measurements, *J. Geophys. Res.*, **94**, 1953–1976, 1989.
- Trampert, J., and J. H. Woodhouse, Global phase velocity of Love and Rayleigh waves between 40 and 150 seconds, *Geophys. J. Int.*, **122**, 675–690, 1995.
- Trampert, J., and J. H. Woodhouse, Assessment of global phase velocity models, *Geophys. J. Int.*, *In Press*, 2000.
- Wong, Y. K., Upper mantle heterogeneity from phase and amplitude data of mantle waves, PhD Thesis, Harvard University, Cambridge, Massachusetts, 1989.
- Woodhouse, J. H., and Y. K. Wong, Amplitude, phase and path anomalies of mantle waves, *Geophys. J. R. astr. Soc.*, **87**, 753–773, 1986.

M. Billien and Jean-Jacques Lévêque, EOST, 5 rue René Descartes, F-67084 Strasbourg cedex, France, (e-mail: Magali.Billien@eost.u-strasbg.fr)

J. Trampert, Department of Geophysics, Utrecht University, PO Box 80.021, 3508 TA Utrecht, The Netherlands

(Received January 1, 2000; revised September 18, 2000; accepted September 26, 2000.)